Materials Science in Semiconductor Processing 37 (2015) 223–228

Contents lists available at ScienceDirect

Materials Science in Semiconductor Processing

journal homepage: www.elsevier.com/locate/mssp

Photothermal study of RF-plasma polymerized hexamethyldisilazane thin films

J.L. Jiménez-Pérez [a,*], M.A. Algatti [b], V. Cruz San Martin [c], P.W.P. Moreira Júnior [b], R.R.P. Mota [b], Z.N. Correa Pacheco [a], A. Cruz-Orea [d], J.F. Sánchez Ramírez [e]

[a] Unidad Profesional Interdisciplinaria en Ingeniería y Tecnologías Avanzadas, Avenida Instituto Politécnico Nacional No. 2580, Colonia Barrio la Laguna Ticomán Delegación Gustavo A. Madero, C.P. 07340 México D.F., México
[b] FEG-DFQ-UNESP, Campus de Guaratinguetá, Av. Ariberto Pereira da Cunha 333, CEP: 12516-410 Guaratinguetá, S.P., Brazil
[c] Escuela Superior de Física y Matemáticas, Av. Instituto Politécnico Nacional S/N Col. San Pedro Zacatenco, C.P. 07738 México, D.F., México
[d] Departamento de Física, Centro de Investigación y de Estudios Avanzados del Instituto Politécnico Nacional, Av. Instituto Politécnico Nacional 2508 Col. San Pedro Zacatenco. Apartado postal 14-740, C.P. 07360 México, D.F., México
[e] Centro de Investigación en Biotecnología Aplicada, Ex-Hacienda San Juan Molino Carretera Estatal Tecuexcomac-Tepetitla Km 1.5, Tlaxcala C.P. 90700, México

ARTICLE INFO

Available online 22 April 2015

Keywords:
Mirage effect
Photo-thermal beam deflection
Plasma-polymerized hexamethyldisilazane films
Thermal diffusivity

ABSTRACT

Plasma polymerization by RF excited low pressure plasmas is a powerful technique for synthesizing thin films for a wide range of applications such in microelectronics, biomaterials and aeronautical industries. Among these applications plasma polymerized hexamethyldisilazane (HMDSN here in) is a promising material due its biocompatibility, optical and electrical properties. In the present paper, we reported the thermal diffusivity measurements of plasma polymerized HMDSN thin films using the probe beam deflection technique (PBD). The samples are thermally thin and optically transparent, with thicknesses ranging from 170 to 600 nm, difficulting their thermal characterization by other photo-thermal techniques (photoacoustic and pyroelectric). PBD measurements were carried out with a diode (20 mW, λ=640 nm) and a HeNe (0.9 mW, λ=632 nm) laser, used as pump source and probe beam, respectively. The probe beam was focused close to the sample surface and its direction was perpendicular to the pump beam. The transverse PBD in skimming configuration is employed and the deflection signal is analyzed using the phase method for the determination of thermal diffusivity. The results show the decreasing of thermal diffusivity with the decreasing of film thickness. HMDSN film's thermal diffusivity values are reported in this paper for the first time being in the range of typical polymeric samples.

1. Introduction

The glow discharge generated in low pressure atmospheres, excited by radio-frequency (usually 13.56 MHz), have been widely used in different processes of scientific and technological interest involving the synthesis of new materials and surface treatment [1–15]. The reason why glow discharges have been widely employed in the technological process is due to the fact that they allow the synthesis of new materials with high quality, attractive prices, allowing the emergence of viable alternatives for making and/or synthesis of materials that already exist [1–5]. The importance of plasma processes can be evaluated when considering the amount of resource applied in so-called advanced processes of synthesis and processing of materials. These amounts of resources reach the tens of billions of dollars per

* Corresponding author.
E-mail address: jimenezp@fis.cinvestav.mx (J.L. Jiménez-Pérez).

http://dx.doi.org/10.1016/j.mssp.2015.03.035
1369-8001/

year worldwide [3,4]. The resources are concentrated mainly in the processes oriented for the synthesis of new and more efficient materials [2–5]. The plasma assisted manufacturing includes a wide range of applications, among which we can mention [4–16]: production of biocompatible materials for surgical implants, ophthalmic implants and drug packaging materials and foods, plasma sterilization of materials sensitive to high temperatures, treatment of polymers and plastics in order to via changes in plasma properties of permoselectivity, coating surfaces with corrosion-resistant materials and synthesis of nano-structured materials and so on. Although the optical and dielectric properties of various plasma-polymerized films are reported from time to time, the thermal properties remain relatively unexplored. This can be attributed to the low magnitude of the thermal conduction parameters of polymers, which makes the measurement difficult [17–28]. The present paper reports the thermal diffusivity of polymeric thin films of hexamethyldisilazane (HMDSN) prepared by low pressure RF-excited plasmas [15,16], using the transverse probe beam deflection (PBD) technique or mirage technique, which is based on the periodical heating of a sample by a modulated pump laser beam. The heat diffusion in the sample produces a temporarily varying gradient of the refractive index of the surrounding medium, which can be detected by the deflection of a probe laser beam traveling in the air layer or liquid medium very near to the sample surface (transverse PBD configuration). The deflection angle, which has amplitude and a phase, provides information about the thermal diffusivity of the sample [17–22].

2. Theory

In this case the probe beam is moved with respect to the pump beam axis by a given offset y and the phase of the deflection angle in the parallel plane to the surface of the sample (transverse component) is measured as a function of y. In this study, we use a probe beam traveling through the liquid nearly at the top of the sample, while a time modulated pump beam impinges on the sample, perpendicular to its surface (Fig. 1). The probe beam is deflected from its trajectory by an angle Φ given by [17]:

$$\Phi = \frac{1}{n}\frac{dn}{dT}\int_{path} \nabla_t T(r,t)ds \tag{1}$$

n being the surrounding medium gas refractive index, s the optical path length, and ∇_t is the gradient transverse to the propagation direction and T is the temperature field distribution. The probe beam has a transverse offset y, with respect to the pump beam axis, and a vertical offset z, with respect to the sample surface. Because of the vertical nature of the deflection one can estimate its lateral or transversal (Φ_t) and normal (Φ_N) component as [17]

$$\Phi_t = \frac{1}{n}\frac{dn}{dT}\int_{-\infty}^{+\infty}\frac{\partial T}{\partial y}dx$$

and

$$\Phi_N = \frac{1}{n}\frac{dn}{dT}\int_{-\infty}^{+\infty}\frac{\partial T}{\partial z}dx$$

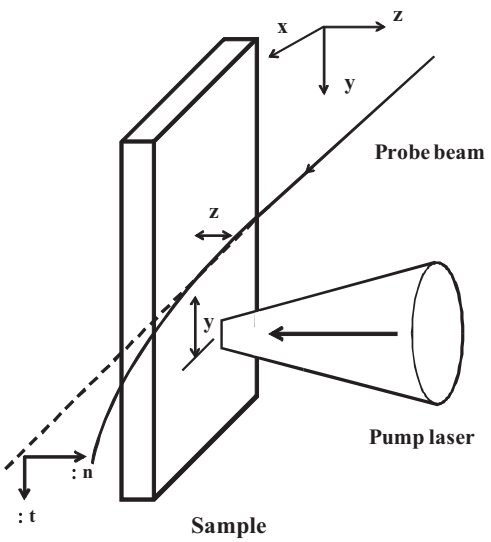

Fig. 1. Photodeflection scheme: normal and lateral components associated to the liquid's refractive index.

The normal and transversal components of the beam deflection show a strong dependence on the air and the sample thermal parameters. The temperature T, due to the pump beam absorption is determined solving the heat equation for each medium, i.e., air or fluid (liquid paraffin), thin film, substrate. In this case we take the model developed by Jackson et al. [18]. Jackson developed a model for three layer system studied with transverse PDS. For this case we have a three layer system which takes into account the glass substrate, the thin film and the liquid paraffin, considering the substrate (Region 2) and liquid (liquid paraffin, Region 0) as thermally thick, i.e. $T_0|_{Z=-\infty}=T_2|_{Z=+\infty}=0$, where the expression for the angular deviation (Φ_t) of the prove beam in the liquid-film is [18]

$$\Phi_t = \frac{1}{2}\frac{\exp(i\omega t)}{n_0}\frac{\partial n}{\partial T}\int_{-\infty}^{-z_0/(\tan\Psi)} dx \times \int_{\infty}^{0}\delta J_0\left(\delta\sqrt{y_0^2+x^2}\right)\beta_0 E(\delta)\exp\{[(\tan\Psi)x+z_0]\beta_0\}\partial\delta + cc. \tag{2}$$

with

$$A(\delta) = -\left[(1-g)(b-r)\exp(-\alpha l) + (g+r)(1+b)\times\exp(\beta_1 l)\right]\Gamma(\delta)/H(\delta)$$

$$B(\delta) = -\left[(1+g)(b-r)\exp(-\alpha l) + (g+r)(1-b)\times\exp(\beta_1 l)\right]\Gamma(\delta)/H(\delta)$$

$$D(\delta) = \Gamma(\delta)\exp(-\alpha l) + A(\delta)\exp(-\beta_1 l) + B(\delta)\exp(\beta_1 l)$$

$$E(\delta) = \Gamma(\delta) + A(\delta) + B(\delta)$$

$$H(\delta) = \left[(1+g)(1+b)\exp(\beta_1 l) - (1-g)(1-b)\times\exp(\beta_1 l)\right]$$

where

$$g = \kappa_0\beta_0/\kappa_1\beta_1 \quad b = \kappa_2\beta_2/\kappa_1\beta_1 \quad r = \alpha/\beta_1$$

Table 1
Parameters used for the simulations. The thermal and optical properties listed below are associated to characteristic values found in glass and thin film [27,28]; for the medium, we used the liquid paraffin properties [29].

Symbol	Parameter	Unit	Value
α_1	Absorption coefficient of thin film	cm^{-1}	2.3×10^{-5}
α_2	Absorption coefficient of substrate	cm^{-1}	1.0×10^{-5}
e_1	Thermal effusivity of thin film	W $s^{1/2}/(cm^2$ K)	0.0280
e_2,	Thermal effusivity of glass substrate	W $s^{1/2}/(cm^2$ K)	0.074
D_0	Thermal diffusivity of liquid paraffin	(cm^2/s)	0.39×10^{-3}
D_1	Thermal diffusivity of thin film	(cm^2/s)	2.23×10^{-3}
D_2	Thermal diffusivity of glass substrate	(cm^2/s)	3.68×10^{-3}
k_1	Thermal conductivity of thin film	W/(cm K)	0.14×10^{-2}
k_2	Thermal conductivity of glass substrate	W/(cm K)	0.45×10^{-2}
l_1	Thin film thickness	cm	0.170×10^{-4}
l_2	Glass substrate thickness	cm	0.09
f	Light modulation frequency	Hz	12.0

Table 2
The parameters of HMDSN films grown at different ion implantation times: thickness and thermal diffusivity (D).

Thickness (nm)	He^+ implantation time (s)	D ($\times10^{-3}$ cm^2/s)
260	15	2.7
257	30	2.66
238	45	2.32
170	60	2.15

and

$$\Gamma(\delta)=\frac{P_\alpha}{\pi^2\kappa_1}\frac{\exp\left[-(\delta a)^2/8\right]}{{\beta_1}^2-\alpha^2}$$

$$\beta_i^2=\delta^2+i\omega/\kappa_i$$

By taking into account the thicknesses, the thermal and optical values of all the components of the three layer system are shown in Table 1 which were calculated by programming the theoretical model of Eq. (2) in Wolfram Mathematica 9.0. The deflection angle, which has amplitude and a phase, provides information about the thermal diffusivity of the sample. The thermal diffusivity D and the thermal conductivity are relate by $k=D\rho C_p$, where ρ is the mass density, C_p is the heat capacity of the sample and $f=\omega/2\pi$ is the modulation frequency of the pumping laser, see also (Table 2).

3. Experimental

Low pressure RF excited HMDSN plasmas were generated within a stainless steel cylindrical, 210 mm of internal diameter and 225 mm long, parallel plate electrodes plasma reactor. The chamber is provided with eight lateral entrances, positioned at the mid plane between the electrodes, that may be used for setting optical, electrical and mass diagnostics and the low (mechanical pump) and high (turbo-molecular pump) vacuum systems. The vacuum inside the plasma chamber is monitored by pirani™ (thermocouple) and penning™ (inverse magnetrom) gauges. The turbo-molecular pump is coupled to the chamber through a gate valve and is used for cleanness purposes. The pressure is pumped down to 10^{-6} Torr, being the chamber purged with argon several times before each running of the experiment. The inner side of the plasma chamber was polished up to the optical quality (roughness of 0.5 μm or less) in order to minimize the retention of impurities and facilitate the cleaning process. The plasma chamber walls were heated with a temperature controlled belt in order to minimize the monomer's condensation as well as the humidity. HMDSN was placed inside a stainless steel bottle and was fed into the plasma chamber through a needle valve. The plasma was excited by a RF power supply operating in 13.56 MHz whose output intensity could be varied from 0 W to 300 W (Tokyo HY-Power model RF-300™). The RF power was coupled to the plasma reactor through an appropriate matching network (Tokyo HY-Power model MB-300™) that allows one to minimize the reflected RF power. The mass spectrometry was performed using a mass spectrometer and energy analyzer (Hiden Analytical model EQP-300™), operating in the mass and energy range from 1 amu to 300 amu and from 0 eV to 100 eV respectively. Mass spectrometry allows one to set the appropriate plasma parameters to keep the monomer's functionalities within the film molecular structure. The block diagram of the experimental setup is presented in Fig. 2. HMDSN films were deposited on microscope glass plates at a constant pressure of 140 mTorr for RF power of 5 W and 30 W. The deposition time varied from 2 to 4 h. The typical film thickness varied from 1000 Å to 2000 Å. After deposition HMDSN films were submitted to a He plasma immersion ion implantion process (PIII) in the same plasma chamber for ion implantation time varying from 15 to 60 min. He-PIII is performed in order to increase the plasma polymerized thin films crosslinking at surface that enhances its stability against ageing effects [15].

The experimental setup used for film's thermal diffusivity measurements is presented in Fig. 3. HMDSN films deposited on glass substrate are fixed in a quartz cuvette. A diode laser operating at the wavelength of 634 nm with 20 mW of output power is used as a pumping source. The pump beam is intensity modulated using a lock-in-amplifier and then focused (~19.0 μm) onto the sample surface. The probe beam, which is focused (~4.0 μm) propagates perpendicularly to the pump beam, grazing the sample surface. The prove laser was mounted on a motorized stage which moves the prove beam in the y direction without have an absolute zero position. The deflection of the probe beam is detected using a bi-cell

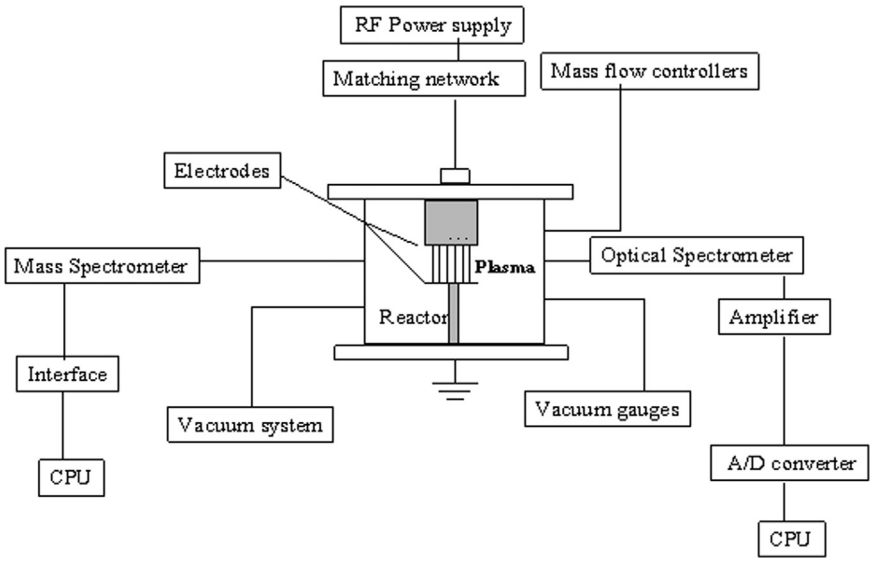

Fig. 2. Schematic diagram of the experimental setup used for plasma deposition of HMDSN films.

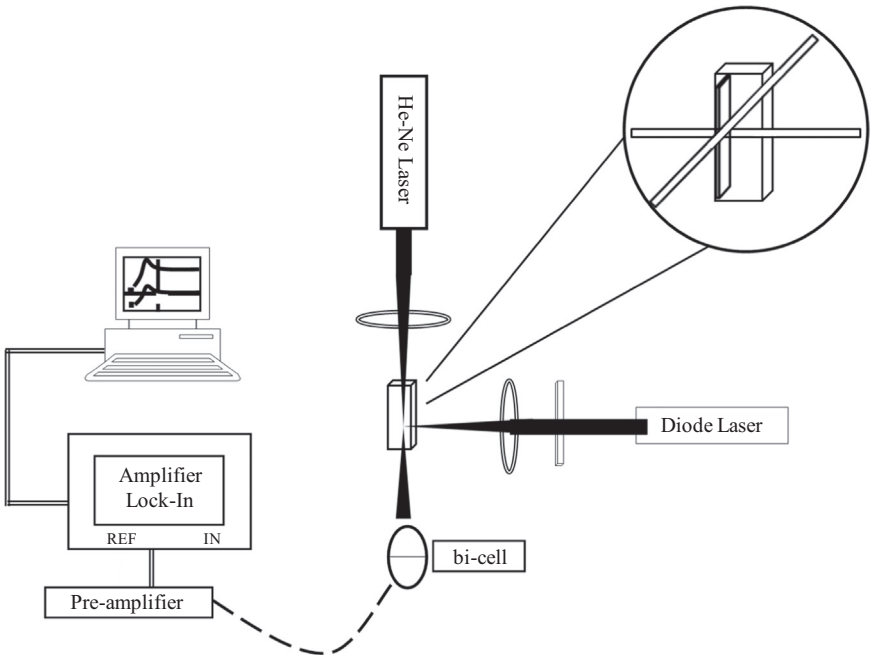

Fig. 3. Schematic diagram of the experimental setup for thermal diffusivity measurements.

(Newport). The signal is amplified using a low noise home-made pre-amplifier circuit and is fed into a lock-in-amplifier (Stanford Research model) from which amplitude and phase of the deflected signal is obtained. The probe laser and its focusing lens are fixed on aluminum flat.

4. Results and discussion

The PBD setup is initially standardized by measuring the thermal diffusivity of pure water. The value of thermal diffusivity is obtained from the linear fitting of the signal phase shift dependence on y offset. It is obtained the value of $D = 1.51 \times 10^{-3}$ cm^2/s, which is quite similar to the value presented on current literature (1.4×10^{-3} cm^2/s) [24]. One important issue to be addressed in a PBD method is the influence of the coupling media on photothermal signal generation [22]. Therefore one performed the thermal diffusivity measurements of liquid paraffin that was used as a coupling media in the present experiment. The obtained results show that thermal diffusivity is $D_{lp} = 2.6 \times 10^{-4}$ cm^2/s. This relatively low value of the coupling media contributes to the photothermal signal in the present experiment [22–25]. Fig. 4 shows the signal phase as a function of the pump-probe offset at a fixed modulation frequency of 12 Hz for HMDSN films treated by He PIII during 60 min. The obtained value for D is 2.15×10^{-3} cm^2/s. The solid line in Fig. 4 shows the

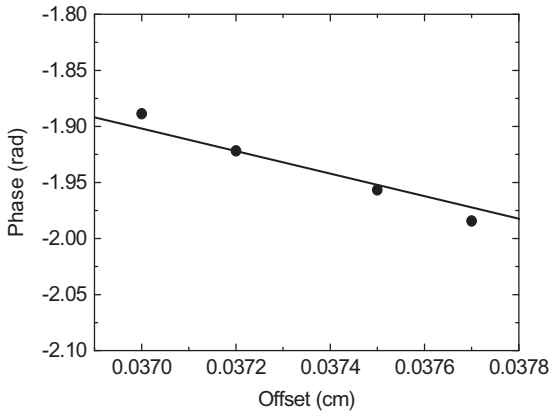

Fig. 4. Phase signal offset for HMDSN thin films with 60 min of He ion implantation.

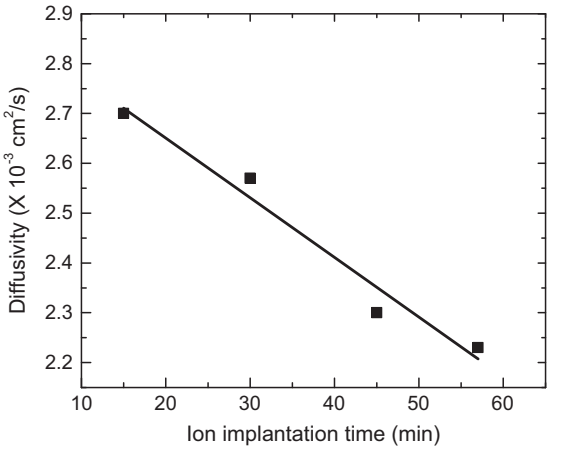

Fig. 5. Thermal diffusivity evolution with ion implantation time.

numerical simulation of the phase of theoretical expression (Eq. (2), taking into account the glass substrate and liquid paraffin as thermally thick) and compared with the obtained phase experimental data (solid circles). The same analysis was carried out for He PIII treated samples during 30 and 15 min. The obtained results show that thermal diffusivity is equal to 2.66×10^{-3} cm^2/s and 2.7×10^{-3} cm^2/s for 30 and 15 min of He PIII treatment respectively. Table 2 presents the average values of D taken for five measurements for samples submitted to different He^+ implantation times. The thermal diffusivity generally decreases with increasing of the ion implantation time as can be shown in Fig. 5. We can also observe in Fig. 6, the growth of the thermal diffusivity with film's thickness. The possible explanation for this behavior is that the He PIII processes contributed for the increasing of polymeric film cross-linking and the decreasing of the film thickness due surface ion sputtering process. The decreasing of film thickness increases the role of the interface film-substrate in the heat diffusion process due interference mechanisms on phonons and electrons for heat transfer. Therefore the thermal impedance seems to increase with the decreasing of the film thickness. Such behavior of thermal diffusivity of thin films was already presented in the literature for different kind of films [28]. Thermal diffusivity of RF plasma polymerized HMDSN thin film sample is reported for the first time and therefore could not be compared with any reported value. However, the measured values lie in the range of polymeric samples [25,30,31].

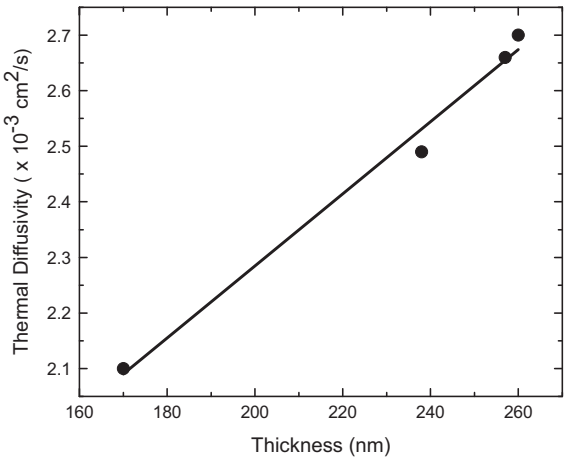

Fig. 6. Thermal diffusivity evolution with film thickness.

5. Conclusions

In this work polymeric thin films of HMDSN with thickness varying from 170 to 600 nm were grown by plasma deposition and thermal diffusivity was successfully measured using a PBD technique in spite of the sample's low thickness and transparency. In the PBD technique liquid paraffin was used as a coupling medium. The substrate influences the heat diffusion in the thin film and the experimental data have a good correspondence with the theoretical model of Jackson et al. The thermal diffusivity generally decreases with increasing of He ion implantation time. This behavior of thermal diffusivity was attributed to interference mechanisms at the interface film-substrate. The thermal characterization of these plasma polymerized films is important for further applications in synthesis of nano-structured plasma polymerized films [11–13,16].

Acknowledgments

The authors would like to thank CONACYT, ICyTDF, COFAA, CLAF and SIP-IPN, México for partial financial support. One of us, M. A. A., also would like to thank FUNDUNESP-Brazil for financial support.

References

[1] A. Fridman, Plasma Chemistry, Cambridge University Press, USA, 2008.
[2] K. Ostrikov, S. Xu, Plasma-Aided Nanofabrication – From Plasma Sources to Nanoassembly, Wiley-VCH, Berlin, 2007.

[3] 2nd ed. R. Hippler, S. Pfau, M. Schmidt, K. Schoenbach (Eds.), Low Temperature Plasma Physics – Fundamental Aspects and Applications, vols.1 and 2, Wiley-VCH, Berlin, 2008.
[4] R. d'Agostino, P. Favia, Y. Kawai, H. Ikegami, N. Sato, F. Arefi-Konsari (Eds.), Advanced Plasma Technology, Wiley-VCH, Berlin, 2008.
[5] H. Biederman (Ed.), Plasma Polymer Films, Imperial College Press, London, 2004.
[6] P.K. Chu, J.Y. Chen, L.P. Wang., N. Huang, Mater. Sci. Eng. R 36 (2002) 143–206.
[7] D.G. Castner, B.D. Ratner, Surf. Sci. 500 (2002) 28–60.
[8] B.D. Ratner, A.S. Hoffman, F.J. Shoen, J.E. Lemons (Eds.), Biomaterials Science: An Introduction to Materials in Medicine, 2nd ed. Elsevier Science, New York, 2004.
[9] I. Bertóti, A. Tóth, M. Mohai, J. Szépvölgyi, Surf. Coat. Technol. 206 (2011) 630–639.
[10] H. Biederman, Surf. Coat. Technol. 205 (2011) S10–S14.
[11] T.S. Santra, T.K. Bhattacharyya, P. Patel, F.G. Tseng, T.K. Barik, Surf. Coat. Technol. 206 (2011) 228–233.
[12] R. Wei, C. Rincon, E. Langa, J. Vac. Sci. Technol. A 28 (2010) 1126–1132.
[13] H. Hody, J.J. Pireaux, P. Choquet, M.M. Couranjou, Surf. Coat. Technol. 205 (2010) 22–29.
[14] F. Kraus, S. Cruz, J. Müller, Sens. Actuators B Chem. 88 (2003) 300–311.
[15] M.A. Algatti, R.P. Mota, R.G.S. Batocki, D.C.R. Santos, T.J. Nicoleti, K. G. Kostov, R.Y. Honda, M.E. Kayama, P.A.P. Nascente, Acta Technol. 56 (2011) T228–T237.
[16] S. Plog, J. Schneider, M. Walker, A. Schulz, U. Stroth, Surf. Coat. Technol. 205 (2011) S165–S170.
[17] M. Bertolotti, R. Li Voti, G. Liakhou, C. Sibilia, Rev. Sci. Instrum. 64 (1993) 1576–1583.
[18] W.B. Jackson, N.M. Amer, A.C. Boccara, D. Fournier, Appl. Opt. 20 (1981) 1333–1344.
[19] Preethy Chirukandath Menon, Ravindran Nair Rajesh, Christ Glorieux, Rev. Sci. Instrum. 80 (2009) 054904-1–054904-9.
[20] J.F. Sánchez Ramírez, J.L. Jiménez Pérez, R. Carbajal Valdez, A. Cruz Orea, R. Gutiérrez Fuentes, J.L. Herrera-Pérez, Int. J. Thermophys. 27 (2006) 1181–1188.
[21] J. Carels, C. Glorieux, J. Thoen, Rev. Sci. Instrum. 69 (1998) 2452–2458.
[22] D.P. Almond, P.M. Patel, Photothermal Science and Techniques, Chapman & Hall, UK, 1996.
[23] R. Gutiérrez Fuentes, J.F. Sánchez Ramírez, J.L. Jiménez Pérez, J. A. Pescador Rojas, E. Ramón Gallegos, A. Cruz Orea, Int. J. Thermophys. 28 (2007) 1048–1055.
[24] R. Gutiérrez Fuentes, J.F. Sánchez Ramírez, J.L. Jiménez Pérez, A. Cruz Orea, Rev. Mex. Fis. 53 (2007) 13–17.
[25] J.L. Jiménez Pérez, J.F. Sánchez Ramírez, A. Cruz Orea, R. Gutiérrez Fuentes, D. Cornejo Monrroy, G.A. López Muñoz, J. Nano Res. 9 (2010) 55–60.
[26] S.M. Shibli, A.L.L. Dantas, A. Bee, Braz. J. Phys. 31 (2001) 418–422.
[27] Wang Xian-Ju, Li Xin-Fang, Chin. Phys. Lett. 26 (2009) 056601-1–056601-4.
[28] H.J. Kim, J.H. Kim, P.S. Jeon, J. Yoo, J. Mech. Sci. Technol. 23 (2009) 2514–2520.
[29] D.R. Lide, CRC Hanbook of Chemistry and Physics, 88th ed. CRC Press, Cleveland, 1977.
[30] A. Cruz Orea, F. Sánchez Sinencio, M.A. Algatti, J.L. Jiménez Pérez, Z. N. Correa Pacheco, A. Garcia Quiroz, Trends Heat Mass Transf. 13 (2013) 51–55.
[31] J. Ravi, B. Syamalakumari, U. John, K.P.R. Nair, T.M.A. Rasheed, J. Mater. Sci. Lett. 22 (2003) 1073–1075.